5-2019

Design and Analysis of a Spatial Neutron Modulator for Neutron Imaging via Compressive Sensing

Daniel Taylor Garza
University of Tennessee, dgarza2@vols.utk.edu

To the Graduate Council:

I am submitting herewith a thesis written by Daniel Taylor Garza entitled "Design and Analysis of a Spatial Neutron Modulator for Neutron Imaging via Compressive Sensing." I have examined the final electronic copy of this thesis for form and content and recommend that it be accepted in partial fulfillment of the requirements for the degree of Master of Science, with a major in Mechanical Engineering.

William R. Hamel, Major Professor

We have read this thesis and recommend its acceptance:

Jindong Tan, Eric Wade, Stephen Jesse

Accepted for the Council:
Dixie L. Thompson

Vice Provost and Dean of the Graduate School

(Original signatures are on file with official student records.)

Design and Analysis of a Spatial Neutron Modulator for Neutron Imaging via Compressive Sensing

A Thesis Presented for the

Master of Science

Degree

The University of Tennessee, Knoxville

Daniel Taylor Garza

May 2019

Acknowledgements

First, I would like to thank my advisor Dr. Bill Hamel. His mentorship while in graduate school has been invaluable. In the lab, we continually benefit from Dr. Hamel pushing us to think more critically about possible solutions that had not been considered. I would also like to thank my committee members, Dr. Jindong Tan and Dr. Eric Wade, for reviewing my work.

Additionally, I would like to thank everyone at ORNL who has helped to make this project possible. Yongqiang Cheng for help in understanding neutron spectroscopy and the necessary design features to ensure successful neutron imaging. Stephen Jesse for all his guidance and feedback with the design itself and continually providing knowledge of how compressive sensing works and how that ties into the design. Raphael Pooser and Phil Evans for their help with understanding optical experiments as well as providing the laser lab training.

I would also like to express my sincerest appreciation to the people who had a hands-on part during this project. Patrick Ellis who is also in Dr. Hamel's lab and has helped through the entire process and has spent a considerable amount of his time ensuring the completion of the project. Jason Schaake who helped both with the optical setup as well as answering any questions I had throughout the experiment was a tremendous aid in completion of the test. Danny Graham who played a critical role in the machining of multiple parts that we needed in order to assemble the prototype including the ring gears and shaft extender.

Finally, I want to thank my family and friends for the support they have offered while working on this project. I am incredibly blessed to have such a caring team behind me.

Abstract

The ability to characterize materials is an important aspect when performing any sort of materials science experiment. When performing studies where understanding the molecular-level characteristics are critical such as for molecular bonding in batteries or complex polymers, analysis techniques such as vibrational spectroscopy are often used. At the Spallation Neutron Source at Oak Ridge National Laboratory the VISION instrument performs vibrational spectroscopy using neutrons. The reason for utilizing neutrons includes aspects such as increased penetration depth into the sample and high sensitivity; however, currently it is only possible to perform bulk sample measurements. By utilizing a technique known as compressive sensing it will be made possible to map material properties and characteristics across an entire sample.

This thesis discusses the design process for creating a spatial neutron modulator that will allow for compressive sensing to be used within VISION as well as the creation of a testable prototype and analysis of the prototype's performance. In order to test the performance of the system as well as the compressive sensing algorithm the prototype is tested using an optical set-up. This approach allows for the concepts to be tested on a cheaper scale to ensure feasibility of the design and compressive sensing algorithm prior to the creation of the final system.

Table of Contents

List of Figures

Chapter 1: Introduction

1.1 Background

Vibrational spectroscopy is a non-destructive identification technique that uses characteristic vibrational spectra to analyze samples. Common vibrational spectroscopic methods include infrared (IR) and Raman, both of which use light beams as the probe [1]. These light beams are in the infrared spectrum for IR spectroscopy but can be infrared, visible, or UV for Raman spectroscopy. Particular molecules have characteristic spectra involving both frequency and intensity for both the IR and Raman spectra. These can be used to determine molecular structure via modeling techniques or to determine compositions of substances since the intensity of each characteristic spectra is proportional to the percentage of the corresponding molecule [2]. Within Raman spectroscopy there are several different techniques such as surface-enhanced Raman spectroscopy, confocal Raman microscopy, coherent anti-Stokes Raman scattering, and resonance Raman spectroscopy [3],[4],[5],[6]. Although these techniques differ in the way they collect the Raman spectra, similar factors determine how accurate the analysis will be such as high signal-to-noise ratio, instrument stability, and resolution [7]. Because of the relatively easy preparation and analysis as well as the non-destructive nature of the test, these spectroscopic techniques have become increasingly used in a wide variety of fields for material analysis.

One of the stations at the Spallation Neutron Source at Oak Ridge National Laboratory uses a vibrational spectrometer in order to perform characterization studies for a range of fields such as chemistry and materials science. The vibrational spectrometer housed here uses neutrons as the probe for reasons such as high penetration depth and sensitivity. This technique involving neutrons is called inelastic neutron scattering and through the change in energy of a neutron is able to obtain the vibrational spectra for the sample. Figure 1 below is taken from [1] and shows the varying advantages and disadvantages of utilizing neutron spectroscopy.

Advantages of INS	Disadvantages of INS
Absence of selection rules; all vibrations observed	Large samples needed
Sensitivity to isotopic substitution, especially H/D	Lower resolution
Ease of calculation of intensities	Longer experiment time
Penetrating radiation	Low temperature required

Figure 1: Advantages and Disadvantages of Inelastic Neutron Scattering [1]

Currently, due to the lack of an imaging technique for neutrons it is impossible to create a spectral image, i.e., one that maps the spectral response across the sample, and instead only a single bulk measurement of the sample is taken. In order to map the properties across the sample, each pixel must be measured. There are two conceptually easy ways that this can be done. In the first a detector is necessary for each desired pixel and a single measurement is taken over the entire sample wherein each detector has the needed information for the corresponding pixel, this would be a detector array. The other method measures a single pixel of the sample at a time using only one detector and sequentially goes through each pixel, this is a raster scan. Both of these methods have drawbacks: in the first an array of the specific detectors are necessary which may not be possible, and the second method is very slow as it requires the same number of data measurements as the desired pixel count for the final image. An alternative method to solving this problem involves compressive sensing.

Compressive sensing is a technique for reconstructing a signal using fewer samples than is typically required. Typically, when sampling a signal, the sampling rate must be at least twice that of the highest frequency of the signal in order to ensure that all the data is captured; this sampling rate is established by the Nyquist sampling theorem. This can cause problems when sample measurements are costly, such as with neutron experiments, or when the sheer amount of samples necessary is so large that it is computationally expensive. In applications such as these compressive sensing comes into play.

Compressive sensing is performed by utilizing what is known as a sampling matrix and imprinting this matrix onto the signal. One of the key factors that allows for the compressive

sensing technique to work is by utilizing sparsity in signals [8]. Many natural signals including images are inherently sparse, i.e. a majority of the signal is zero in some basis. Another key factor is the sampling matrix used when sampling the signal. In order for the sampling matrix to be effective the sampling matrix must be incoherent with the signal basis, i.e. there is not a relationship between the two. In other words, if the signal is sinusoidal then the sampling matrix could not be formed from a wavelet transform of sine and cosine functions. This presents a problem that in order to determine what form of sampling matrix to use the signal must be known beforehand. To get around this the sampling matrix can be randomly generated as the resulting matrix will be incoherent with the signal with high probability [9].

In single-detector applications the sampling matrix must be imprinted onto the signal, typically light for a camera application but for the final application of this project the matrix must be imprinted onto the neutron beam. In order to do this a spatial modulator is used; a common spatial light modulator (SLM) used is a digital micromirror device (DMD). A DMD contains arrays of actuated mirrors that are able to selectively direct portions of the light, an example of this is shown in Figure 2 below [9]. The set of both sampling matrix and corresponding sampled signal are passed to a compressive sensing algorithm. There are many of these minimization algorithms [10] but they generally work by solving systems of underdetermined linear equations, which have more unknowns than equations. These systems of equations are formed by the sampling matrix and the measurement vector. The assumption of the sparsity of the signal is what allows for the algorithm to solve such a system. Solving these systems allows for the reconstruction of the original signal, which in our case produces an image.

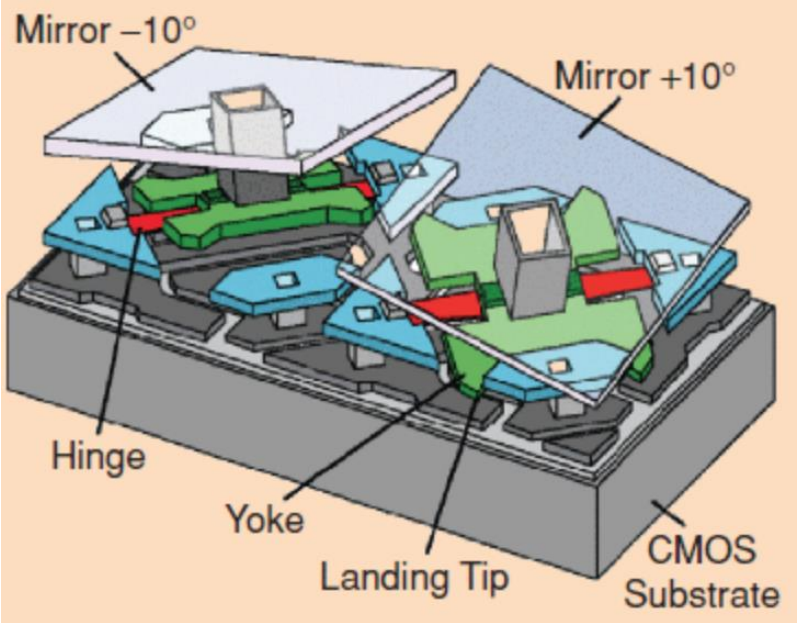

Figure 2: Digital Micromirror Device [9]

1.2 Motivation and Purpose

The overarching goal of this project is the ability to do spectral imaging with neutrons, which provides the ability to map material properties within a sample. By gaining the ability to map molecular characteristics across a sample, new capabilities for materials testing and experimentation will be available. In order to be able to perform spectral imaging with neutrons it is necessary to map a specific spectral measurement at some resolution. Although this can be done by measuring a part of the sample only as large as the resolution, this process is very slow. By utilizing a process called compressive sensing, the total amount of time that is required is cut by two-thirds. Thus, designing a system that enables the compressive sensing algorithm is of critical importance. The purpose of this thesis is the first step in designing that system by creating a functional prototype that illustrates the feasibility of performing compressive sensing using the designed system.

1.3 Scope of Thesis

The scope of this thesis involves the creation of a prototype spatial neutron modulator (SNM) as well as the analysis of the compressive sensing algorithm performance using the

prototype design and the feasibility for its use in VISION. This functional prototype uses lower cost components due to removing the low-temperature and vacuum constraints necessary for the final design. Software components will also be necessary both during the testing as an interface to control the setup, controlling the motor during the testing, and acquiring data for each measurement as well as after testing in order to perform the compressive sensing algorithm on the acquired data.

Chapter 2: Modulator Design

2.1 Overview of Design Criteria

Because the SNM will be used inside of the VISION testing chamber, there are several design requirements and conditions that the system must operate under. First, the SNM will be located at the end of a long sample stick which is inside of a long and relatively narrow hollow cylindric testing chamber; the sample stick can be seen in Figure 3 while the testing chamber can be seen in Figure 4. This cylinder has a diameter of 8.2 centimeters which establishes the maximum width constraints for the SNM. The length of the SNM along the axis does not have a specific design limit.

When the VISION system is in operation the temperatures within the tube are chilled down to 5 Kelvin. The purpose of this cooling is to minimize atomic vibration since this vibration presents itself as noise and sampling error in the vibrational spectroscopy measurements. Thus, the system must operate at this extremely low temperature which poses a serious design constraint such as requiring solid-state lubricants. Additionally, it was desired that the system should be able to operate around room temperature as well. This large change in temperature poses design issues such as considering the thermal expansion and shrinkage as well as using materials that operate well under both temperatures. The VISION testing chamber is also operated under vacuum. Because of the angle that the neutrons scatter from after penetrating the sample, there should not be any components of the system within a 30° angle from the outside edge of the sample.

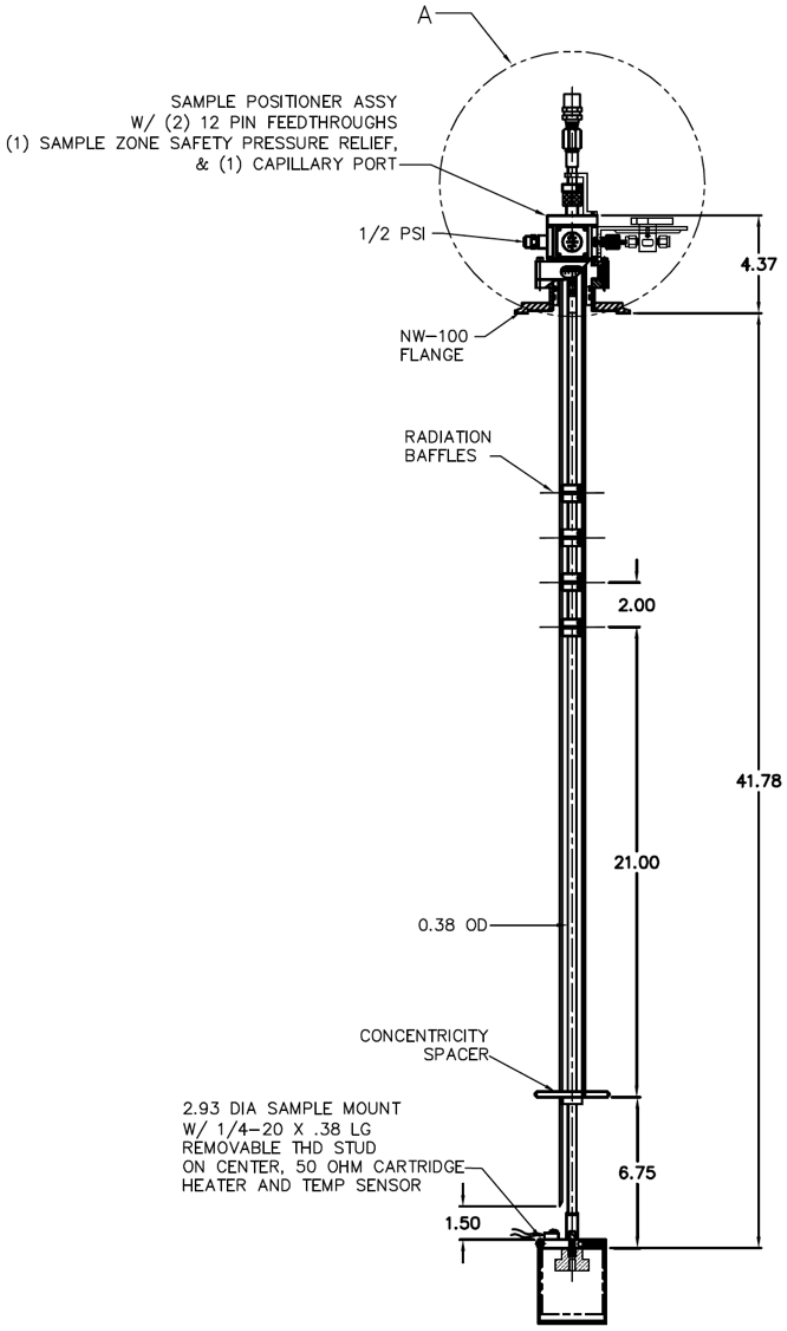

Figure 3: VISION Sample Stick Drawing

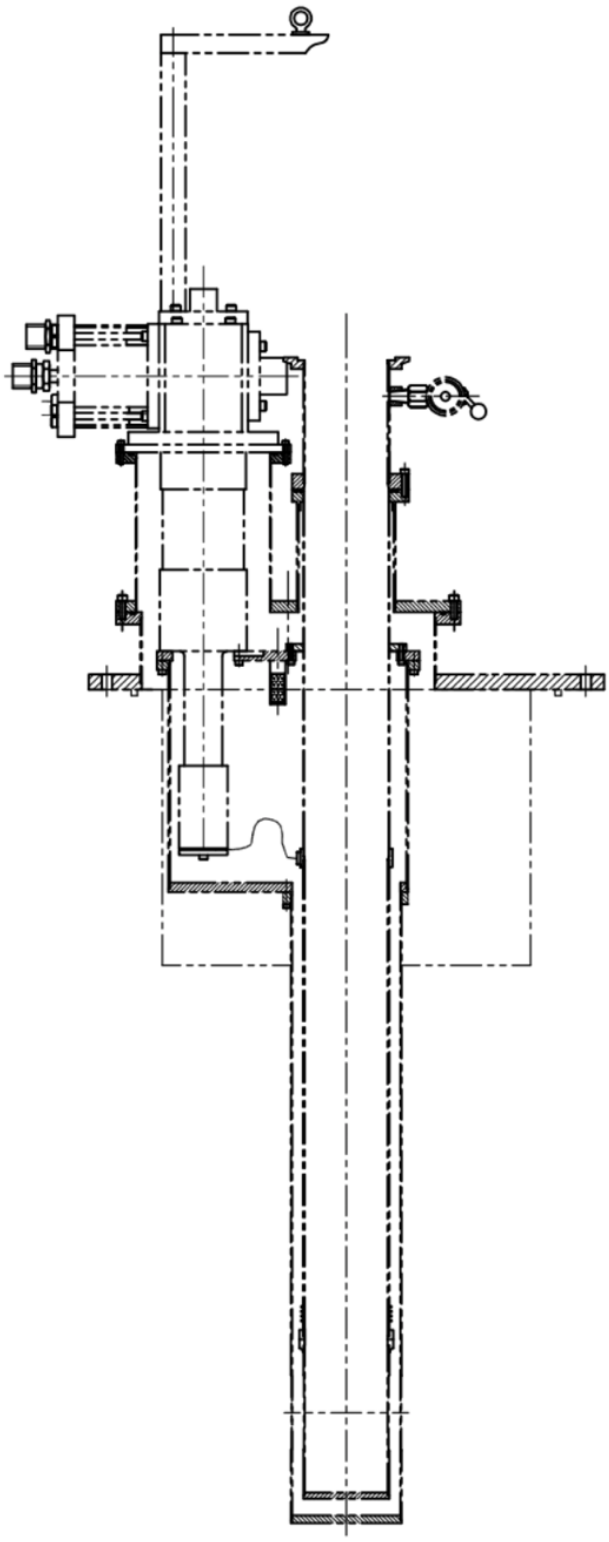

Figure 4: VISION Chamber Drawing

2.2 Concept and Trade-offs

In order to achieve compressive sensing, a few different versions of modulator designs were considered. One major consideration that had to be accounted for in each design is that the pattern of the mask has to be changeable as every configuration needs to be a different "random" matrix as any repeated masks offer no new information for the compressive sensing algorithm. Using this basic concept of needing a modifiable mask several iterations of modulator have been postulated.

A design that had previously been created at ORNL is a small container containing free moving particles [11]. In this experiment, the container holding the particles was laid horizontally and a small electric motor would agitate the particles moving them into a new position. The setup that was used in this experiment can be seen in Figure 5. One disadvantage of this setup was that the smaller particles used during the experiment had the tendency to stick together after the electric motor would agitate the container. Because of this clumping, the randomness of the sampling matrices was decreased, and the overall resolution was lowered. In order to prevent this effect a slight alteration was suggested in which the container would hold two different types of beads: one that is made of a neutron blocking material and one that is made of a neutron transparent material. Similar to the previous design the beads would be agitated to alter their configuration. One way that this was proposed to be done was via several small bursts of air into the container. A depiction of this can be seen in Figure 6 below.

In order to determine what the configuration of the beads is for each sample measurement a mirror would be used to reflect the bead pattern into an optical camera. A few problems with this setup are that the reliability of obtaining new mask configurations for the large number of necessary sample measurements is uncertain as the agitation may not necessarily change the bead positions in enough number of ways. The bead positions are also not controllable and thus an additional optical camera is necessary for this design to work. For the case of neutron imaging in the VISION chamber, the assembly is located in the testing tube which has no light and is in a very tight space limiting the applicability of such a design.

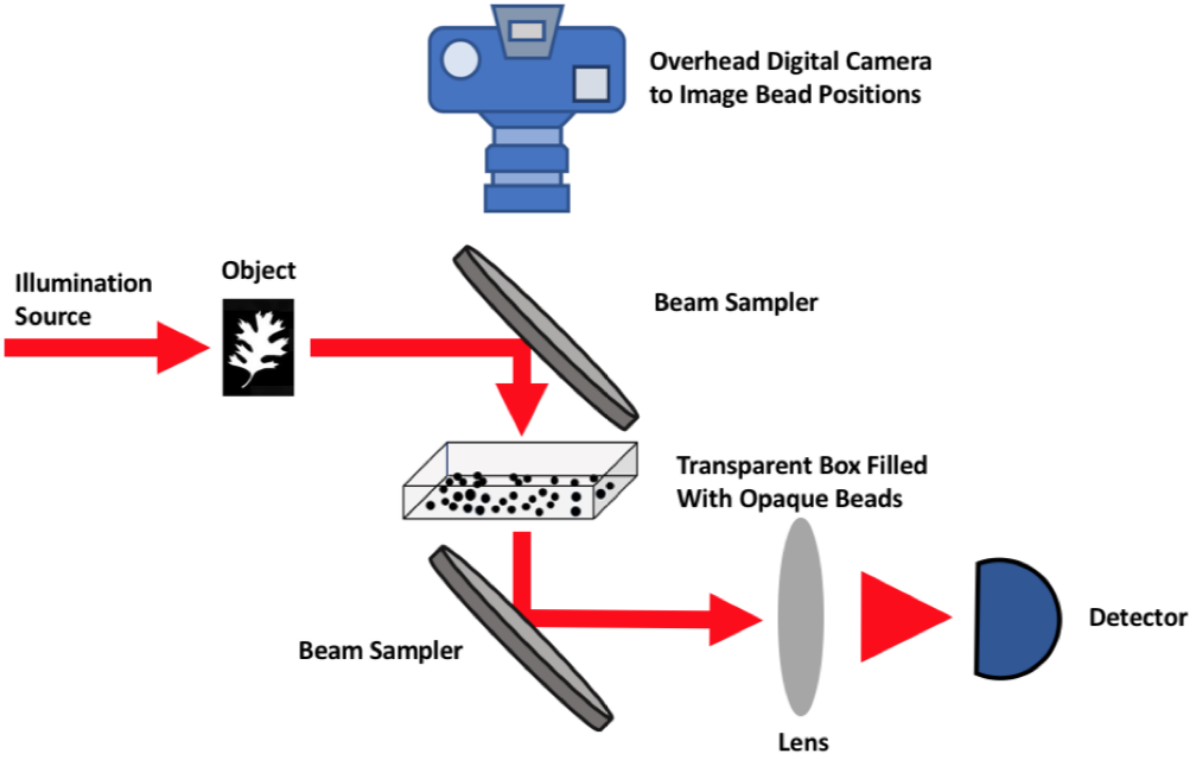

Figure 5: ORNL Imaging Setup

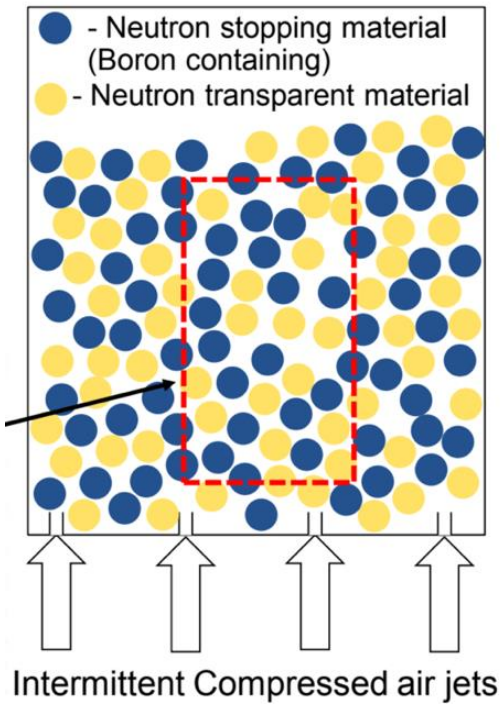

Figure 6: "Box of Rocks" Method

Another design which was proposed at the start of the project is one that utilizes a rigid mask composed of a random grid of both neutron opaque and neutron transparent sections. This mask would have 3 actuated degrees of freedom allowing it to translate in the x and y direction as well as be rotated along the axis perpendicular to the face of the mask. This design would increase the reliability of obtaining unique sampling measurements as well as reduce the necessary space slightly from the original design that needs an optical camera. Although this design is an improvement in the controllability of the SNM as it creates a consistent set of mask configurations that are sampled through as well as allowing for feedback from the motors, it does require three separate motors to actuate the degrees of freedom which is not ideal in the small amount of available space for the SNM.

A similar design was then suggested which also used the idea of a rigid mask pattern; however, this new design used only a single motor which further simplified the design and reduced the space necessary. The mask that was used for this project was an array with 1mm spars running horizontally and vertically with 5x5 mm boxes. A matrix was randomly generated in MATLAB and these boxes were filled according to the resulting matrix; the resulting mask can be seen in Figure 7. This grid design was suggested by Stephen Jesse in the project group. Overall, it provides good structural integrity and is easily modifiable in the box sizes and spar widths. The grid design also allows for the mask to be easily constructed as a randomly generated matrix can be used in a one-to-one relationship where each element in the matrix corresponds to a box in the mask design. However, any random mask design would work and in the future other random designs without a grid system could be utilized. In order to achieve the required number of unique mask configurations, two rotating masks would be used as opposed to a single mask that has 3 degrees of freedom.

These masks would rotate at different speeds so that it would take a large number of revolutions before a similar mask configuration was repeated. Figure 8 and Figure 9 show the predicted mask configuration after 100 iterations with a red box showing the test aperture and a zoomed in shot at the aperture showing the sampling matrix that would be used in the reconstruction algorithm. These predicted mask configurations were based on a MATLAB code that was written for this project. This code takes a provided mask image as well as degree

rotation per step and iterates through the predicted mask configurations as well as accounting for the center offset between the two masks. These predicted configurations were then exported and could be imported as a matrix for use in the reconstruction algorithm; this MATLAB code can be found in the Appendix of this paper. The advantages of this method are similar to the other motor-controlled method in that the mask configurations are easily repeatable and controlled via the encoder feedback while also having an additional advantage in reducing the total space envelope of the device as well as considerable cost reduction due to needing only one motor as opposed to three motors.

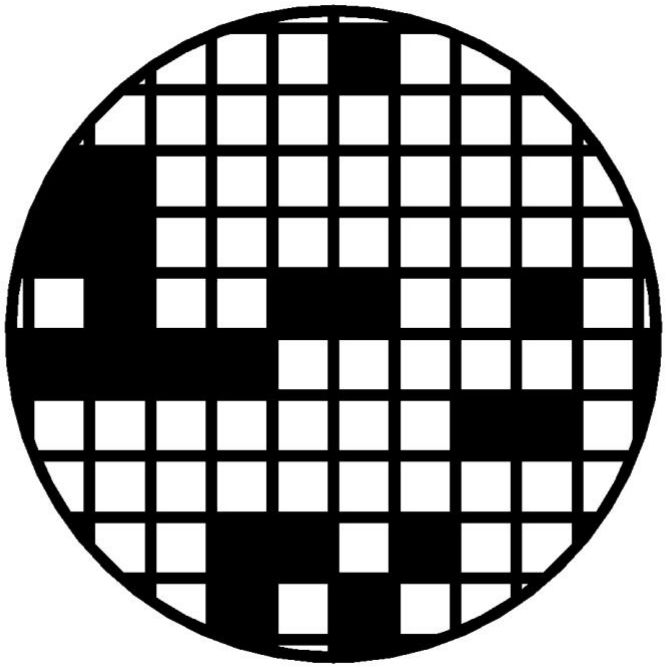

Figure 7: Mask Design

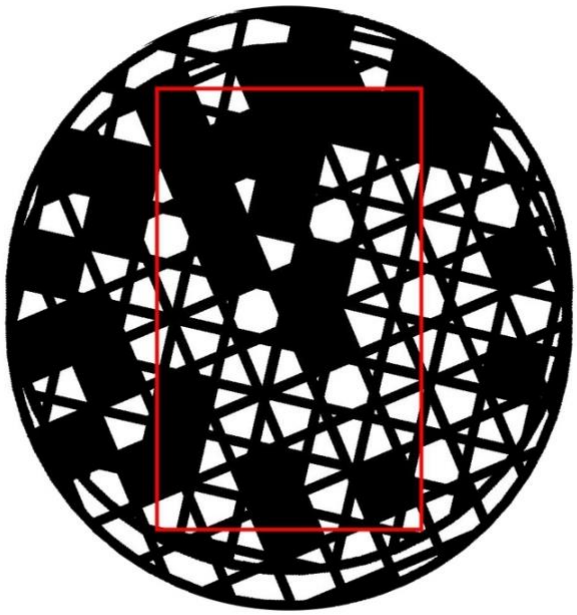

Figure 8: Two-Mask Design showing Aperture at Iteration 100

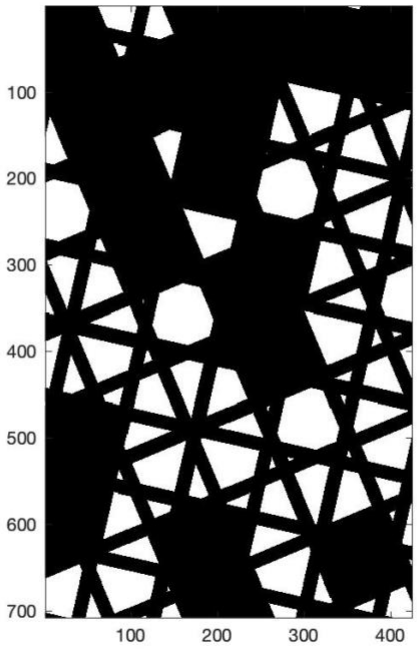

Figure 9: Sampling Matrix for Iteration 100

Due to the various design constraints imposed on this project several design choices were affected that either limited the choices available or had to be made to prevent failure of the design. One of the more limiting constraints was that of the extremely low temperatures as well as the wide range of temperatures the design is expected to operate under. In order to operate under the low temperature restriction, mechanical mask drive train parts are necessary that are compatible with a temperature range from near absolute zero to ambient. These include parts such as ball bearings that are designed with dry lubricants such as molybdenum disulfide or tungsten disulfide as opposed to liquid lubricants that would freeze at these temperatures. Motor choice is also critical, and a small inertial piezo drive was the final motor chosen due to its high precision, low-temperature and vacuum operating conditions, and highly compact size. The low-temperature has a further impact post-testing as the testing stick with the SNM attached has to be removed from the chamber. The entire testing chamber cannot be gradually heated to near room-temperature prior to removal as cooling the chamber back down to 5 Kelvin takes a considerable amount of time. This can cause problems due to the water condensation that will occur when the cold SNM is removed and brought into room-temperature air. Although the water will not cause failure for most of the parts, internal water leakage into the drive motor could lead to its failure. For this reason, a way to locally heat the motor before removal from the chamber had to be implemented. The operating temperature range also introduced problems into the precision parts of the mask drive mechanism due to thermal expansion effects. An initial step that was considered to combat this problem is utilizing homogenous materials for the parts so that the coefficient of thermal expansion is equal across all parts of the system to limit disproportionate expansion across the SNM.

Since the scope of this thesis includes only the design of a feasibility prototype and not the final design for use in the VISION instrument, a key constraint, temperature, can be effectively ignored to reduce cost and lead times. First, since thermal constraints need not be considered, cheaper mechanical components such as the ball bearings and motor can be chosen that operate in more standard ranges. Second, since the prototype will only be operated under normal room-temperature ranges, homogenous materials across the parts are not as necessary. This allows for some of the parts to be additively manufactured and for the

different hardware components to be bought only to size specifications without requiring the materials to match across each.

2.3 Design Iterations

Over the course of the design process additions and refinements were made as the final two-mask design became increasingly refined. The placement of the sample holder was changed early in order to be aligned near the center of the sample stick as the clearest data is obtained when the sample being tested is at that point in the tube due to an approximate 30° scattering once the neutrons hit the sample.

For a similar reason, the initial motor placement also had to be changed. Originally the motor was placed in such a way that the neutron scattering after hitting the sample would also interact with part of the motor. For this reason, the motor in the design for the final system was moved to be between the two plates holding the masks and the plate holding the motor was moved closer to the middle to avoid inference with the neutrons. A hole large enough for the motor base was created in the plate closest to the middle of the modulator so that the motor could attach to the motor plate.

The gear selection for the design was also changed many times during the design process. Originally, the gears were designed with the only attachment method in mind being a keyway in the shaft and gear to prevent rotation. This was in part due to the very low forces involved in this application and slow rotation speeds; however, it was decided that more secure attachment method would be desirable as any system failures can create considerable time delays in the VISION chamber. For this reason, hubbed gears with set screws were decided on as the attachment mechanism. This meant that the empty space between the two main plates had to be increased in order to accommodate the increased width of the hubs.

2.4 Mechanical Design

In order to create good mesh between the gears in the assembly, the top gears are mounted on shafts that have a modifiable distance from the mask gears. This ensures that the correct pitch distance is able to be used to prevent binding. Being able to modify the distance will also be critical in the final application when large thermal differences will be present

causing contraction of the materials when going from room temperature to 5 Kelvin. The ability to modify the center distances gives the user the freedom to set up the system to specifically work under either temperature condition. The bearing plates that the shafts were mounted on to allow for a modifiable center distance can be seen in Figure 10.

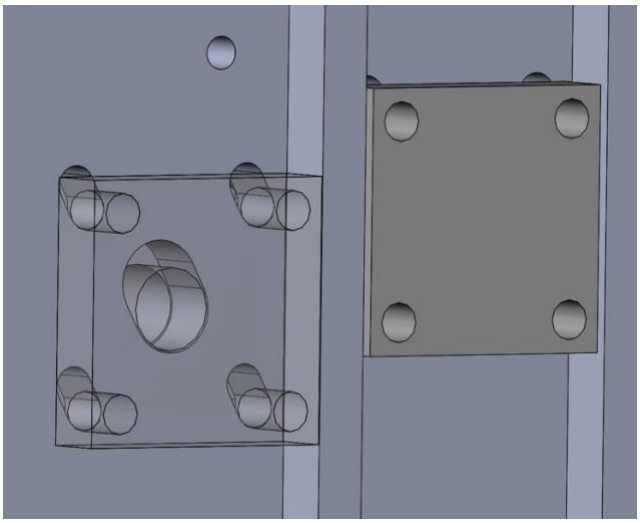

Figure 10: Movable Bearing Plates

Because of the space constraints, the design ended up being much longer, relatively, than it is wide. Due to the plates being pinned on either side and being relatively long and thin, any bending moments could cause significant distortion near the middle of the plates. Since the gears are mounted on these plates the distortion could cause the gears to stop meshing well during use. As this is clearly not desirable for the system several steps were taken to minimize these effects. In order to decrease the overall deflection, we can think about inserting a theoretical point load in the center of the beam, plate in this case, and minimizing the deflection caused by that load. Thus, the equation we are looking at for this situation is a beam with fixed end conditions and a point load at the center:

$$\delta = \frac{F * L^3}{c * E * I}$$

Where F is the applied force, L is the effective length, E is the modulus of elasticity, I is the moment of inertia, and c is a constant.

Since we are trying to decrease the deflection for a given load, the force is not a controllable variable. What we are left with is either decreasing the total length or increasing the stiffness. Although the overall length could not be decreased any more than it already was, what could be done is adding in a cross member to decrease the unsupported length. The cross members that were added can be seen in Figure 11.

In order to increase the stiffness of the plates, options include changing the material or increasing the area moment of inertia. Material selection was limited for the prototype model so the best option is to increase the area moment of inertia; however, tight space constraints prevent simply increasing the width to increase the area moment of inertia. For this reason, the option that was decided upon was to add small reinforcement spars running lengthwise across the plate, which can be seen in Figure 12.

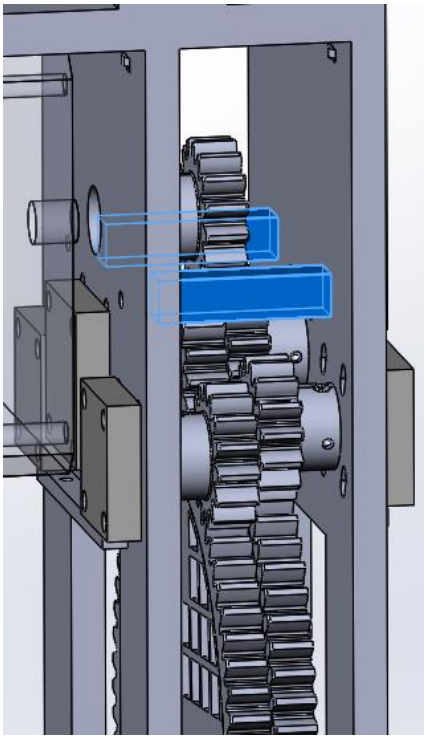

Figure 11: Cross Member Supports

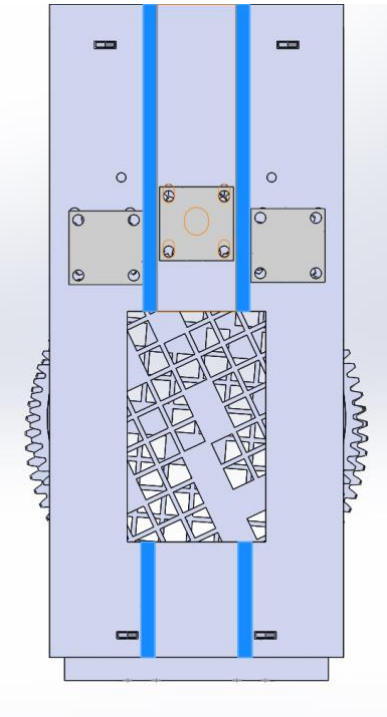

Figure 12: Reinforcement Spars

In order for the compressive sensing algorithm to function, many unique configurations are necessary. For the resolution desired for this stage in the project, a goal to reach was 1000 unique configurations in order to provide proof of concept with a relatively detailed spectral image. To achieve this count with the two-mask design the masks can be rotated at slightly different speeds causing the revolutions of the masks to not be synced. This can be achieved either via separate motors operating the two masks or with a single motor but a different gear ratio between the motor shaft and each mask. Since space constraints are a large issue with this project, using two motors is not a realizable solution. Thus, the gear ratio must be different between the two masks. The two ring gears surrounding the masks have slightly different number of teeth, one with 70 and the other with 72. These gears were chosen as they fully enveloped the dimensions of the aperture while also remaining within the overall space constraints of the project design. Since the input shaft is the same for both gears, for every full revolution of the gear with 72 teeth the gear with 70 teeth will have rotated slightly more than one full revolution. After 168 revolutions of the motor shaft, the 72-toothed gear will have

made 35 revolutions and the 70-toothed gear will have made 36 revolutions and the configurations will begin to repeat. In order to reach 1000 mask configurations, we can calculate the maximum rotation of each mask between tests. (360°/rev)*(35 rev) / 1000 = 12.6° for the 72-toothed gear and 12.96° for the 70-toothed gear. More importantly, the motor shaft will rotate 60.48° between each sample measurement. This information provides the step size for the motor shaft that should be used between each sample iteration in order to achieve the desired number of mask configurations.

2.5 Mechatronics Design

In order to control the modulator positions, a stepper motor was used for the prototype. A small motor controller allows basic control of the motor over several interfaces, among these the USB and TTL serial interfaces were most important for our use. The controller also came with a free software download that allowed for quick motor control via USB connection; the GUI for this software can be seen in Figure 13 below. One unfortunate aspect of this motor was that it did not have an encoder so no feedback was possible to verify the positions. The final design for this project utilizes a motor that has a built-in encoder. This allowed for easy testing of the motor as positions and velocities could be quickly set for the motor. The motor could also be controlled via Python and LabView.

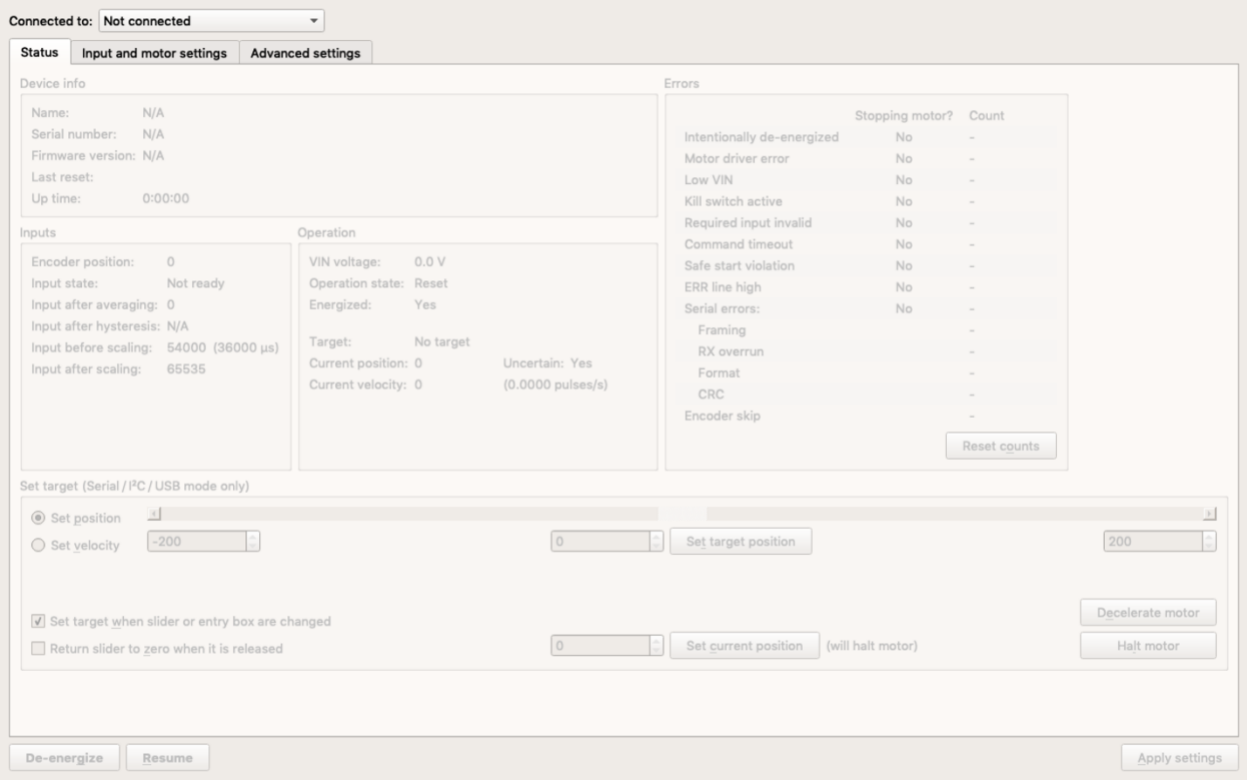

Figure 13: Pololu Motor Controller GUI

2.6 Design Analysis

The assembled prototype can be seen in Figure 14 below. Before experimentation on the optical set-up, the motor and assembly were tested to ensure smooth running of the components. Although it did not cause any problems during the testing phase, one component that could be improved upon was the shaft mounting design. Due to the shaft only being secured on the bearing, the cantilevered design caused some slight dip in the shafts near the gears. The rigidity of the assembly was another initial area of concern, but after the implementation of the cross members the structure became significantly more rigid. The plates that were glued onto the backs of the gears also prevented the mask gears from coming out of alignment.

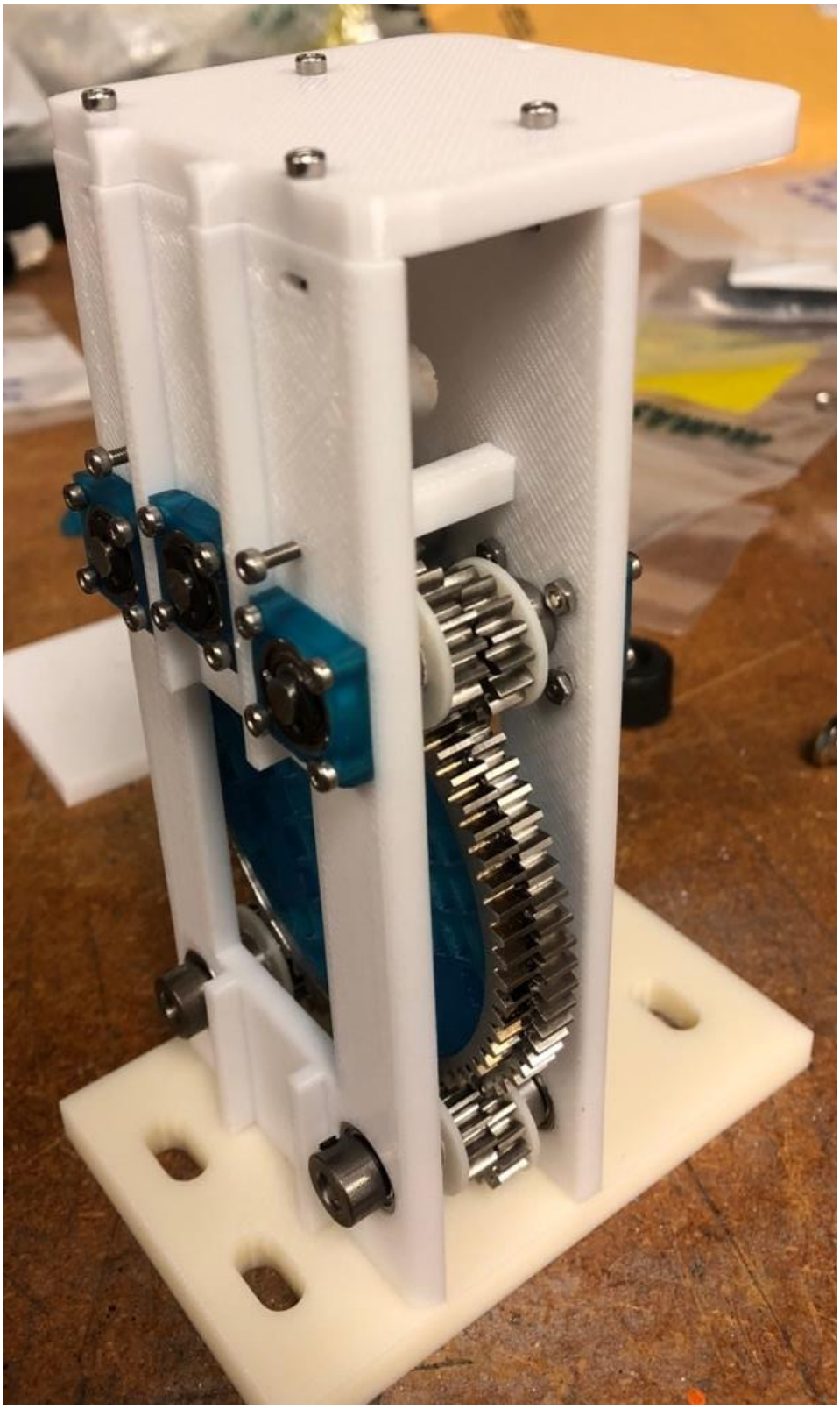

Figure 14: Final Assembly

2.7 Optical Setup

In order to test the viability of the mask design for use in compressive sensing the assembly was tested on an optical bench using light. The setup for the experiment can be seen in Figure 15 and Figure 16 below. The measurement device is a photodiode attached to a 2204A PicoScope. This PicoScope is connected via USB to a computer running Windows OS and the compatible PicoScope software. Using a 64-bit PicoScope SDK this software is connected to a basic LabView program that would take an averaged voltage value for a given number of samples after a specified amount of elapsed time. The light was focused onto the photodiode by the circular lens in front of it, this can also be seen in Figure 16. The motor controller was controlled via the free downloadable Pololu software [12] that interfaced with the motor controller via USB. An initial experiment used a simple LED flashlight run off a battery power-source as the light source. Later optical tests used a 780nm fiber-coupled laser beam which can be seen in Figure 17. As can be seen in Figure 16, what was being imaged by the device during the flashlight experiment was the letter 'N' which was a black sticker placed onto a glass slide in front of the device aperture. Later tests used the letters 'V' and 'X' as well as simply imaging the beam itself. When using the laser beam a lens had to be used as a beam expander when imaging the letter 'X' as the initial beam was not large enough to illuminate the letter. This lens was removed when imaging the beam. After the initial test with the LED flashlight, a camera was used to image the sampling matrix produced by the masks as can be seen in Figure 17.

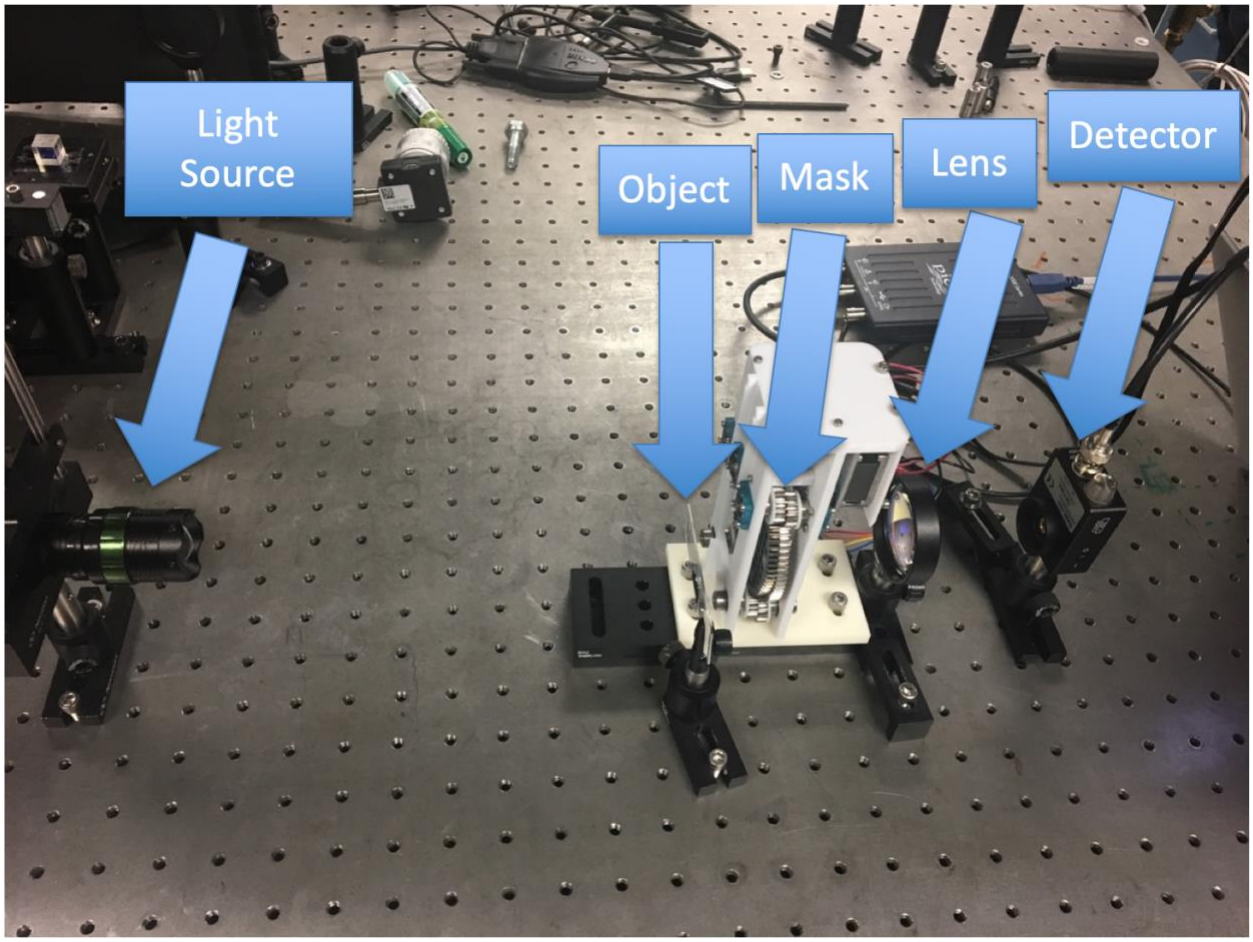

Figure 15: Optical Setup View 1

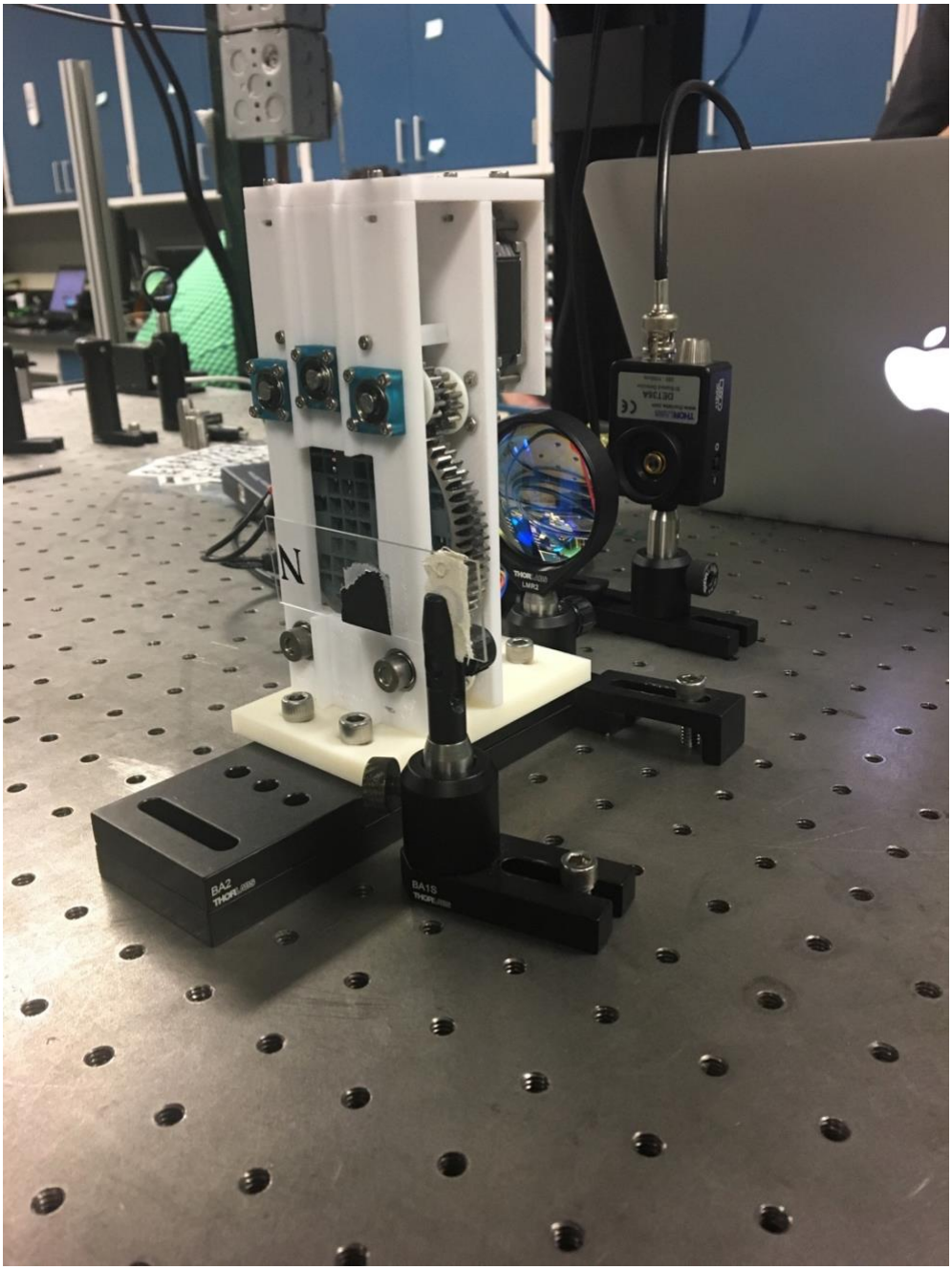

Figure 16: Optical Setup View 2

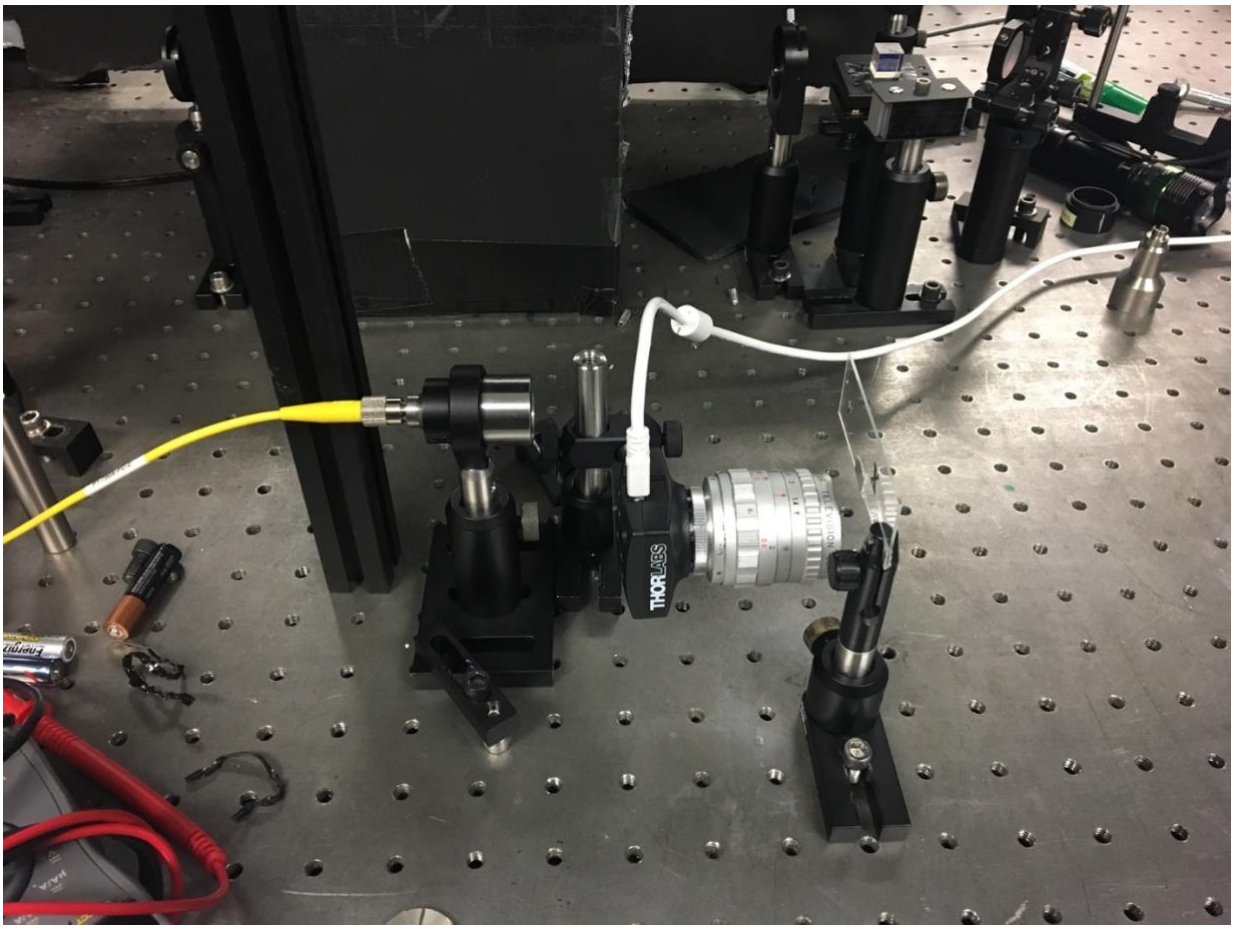

Figure 17: Fiber-Coupled Laser and Camera

Chapter 3: Compressive Sensing Performance Analysis

Four experimental runs were done with different setups for each. The first experiment utilized an LED flashlight as the light source with a black 'N' on a glass slide that was placed in the center of the light that would be imaged. The second experiment utilized a fiber-coupled laser beam as the light source with a small black 'V' to be imaged. The third experiment utilized the same laser but expanded the beam using a lens in order to image a black 'X' that was the same size as the letter used in the first experiment. The fourth experiment once again utilized the laser but this time both the lens and glass slide were removed and only the laser beam was imaged. In each experimental run after the first, a small camera was used to image the sampling matrix. The voltage and sampling matrix data sets were input into a reconstruction algorithm called TVAL3 [13] that would output the reconstructed image.

Unfortunately, the experiment using the flashlight setup was unsuccessful. The image that was reconstructed from this experiment did not resolve correctly. Several problems seemed to contribute to this result. One of the more significant problems was the large variation in light intensity due to the light source. The LED flashlight has significantly more variation in intensity than sources such as the laser sources available in the lab. On its own this could cause the compressive sensing algorithm to fail. The more significant problem with the light source though was that due to the experiment taking approximately five and a half hours of constant operation the battery in the flashlight drained many times and new batteries would have to be replaced. This caused significant peaks and troughs in the data along with a more gradual negative slope over the entire data set that can be seen in Figure 18. Another potential problem was caused by the lack of encoder with the motor. Due to this, the target position of the motor was not necessarily the real position of the motor. Since the reconstruction algorithm depends on the sampling matrix used in the reconstruction algorithm to match with the matrix used during the test, this uncertainty can cause the image reconstruction to not resolve correctly. Because of the inconsistencies in the light intensity delivered by the source, the compressive sensing algorithm used was unsuccessful in reconstructing the correct image.

In order to remedy these effects in the future runs two different things were done. First, a laser-beam was used in place of the flashlight to provide a consistent and reliable light source. Second, a small camera was used to take a picture of the sampling matrix at each configuration.

The second and third experiments had similar results. The voltage values output by the photodiode no longer followed the downward trend from the previous experiment due to the laser that was used, the recorded voltage values over the third experiment can be seen in Figure 19. However, based on the results the resolution of the system was not sufficient to reconstruct the images. In the second experiment a small 'V' was imaged; however, the resolution of the system was not sufficient to resolve the small letter. This was not very surprising as the two arms of the letter were actually smaller in width than the spars of the sampling masks. In the third experiment, the letter 'X' was imaged and the laser beam had to be expanded by a lens. The reconstruction algorithm was able to successfully resolve the light around the letter; however, the interior was still unable to be resolved correctly as can be seen in Figure 20.

In order to simply show a proof of concept for the design system working with the compressive sensing algorithm, a fourth experiment was run. In this run the lens and glass slide were removed and only the gaussian beam was imaged. The algorithm was able to successfully resolve the beam and the reconstructed image can be seen in Figure 21.

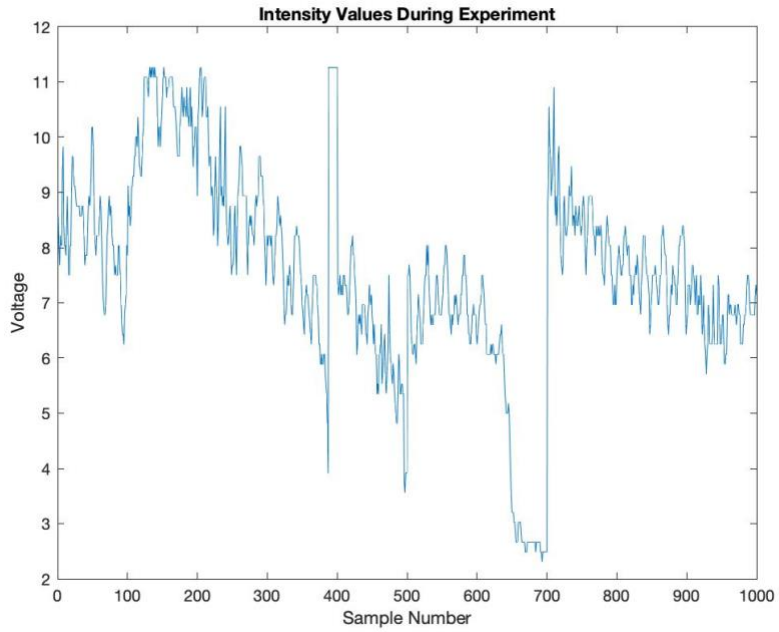

Figure 18: Graph Showing Measured Voltage Values – Test 1

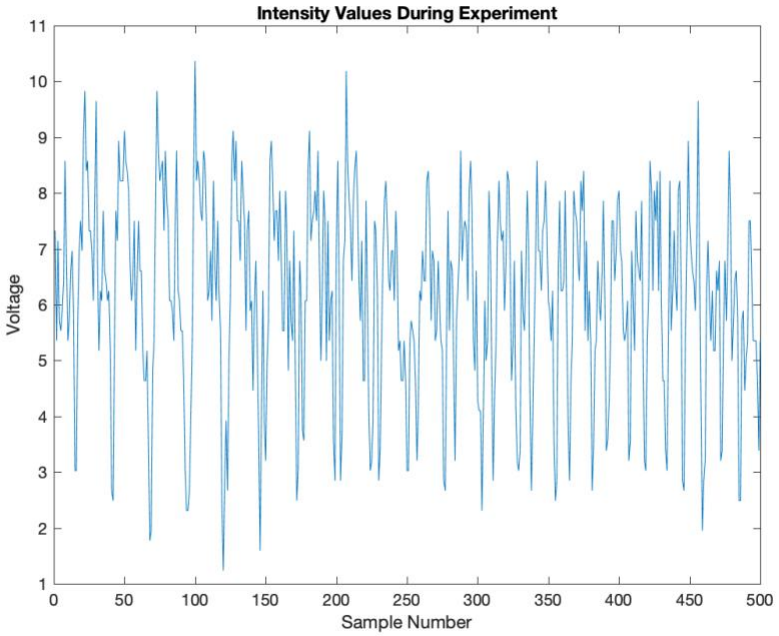

Figure 19: Graph Showing Measured Voltage – Test 3

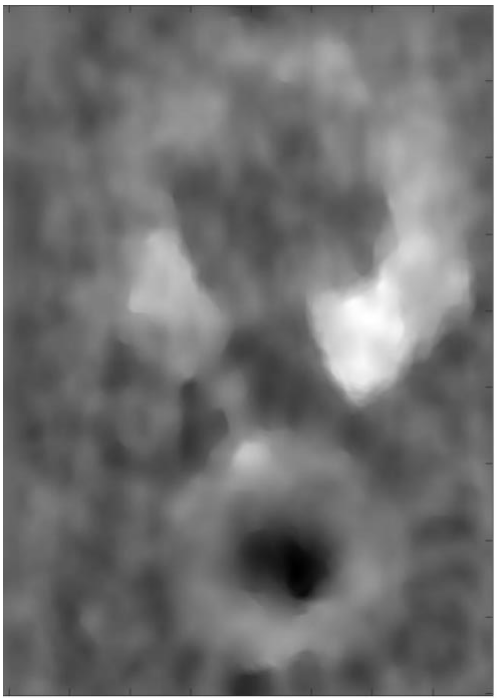

Figure 20: Reconstructed Image of Test 3

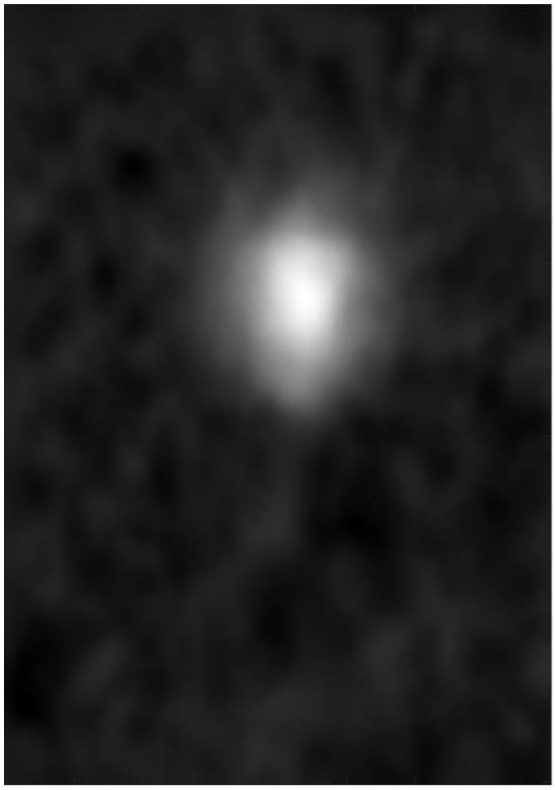

Figure 21: Reconstructed Image of Test 4

Chapter 4: Summary and Conclusions

Overall, the design of the spatial neutron modulator was successful. The finished prototype met the size requirements defined by the VISION tube, had design margins to allow for operation at both room temperature as well as the 5 Kelvin necessary for the neutron tests, and successfully stepped through 1000 different mask configurations. Unfortunately, the initial experiment was unsuccessful; however, this is believed to be more due to the inconsistent light source rather than a design flaw. The fourth test shows that the reconstruction algorithm works correctly with our design. A possible avenue of improvement to the design involves a redesign of the mask used in this experiment. Because of the design of the mask, it has spars running along the entire length of it both horizontally and vertically at regular intervals. This design reduces some of the randomness. It also appears to introduce a small portion of the aperture that is always covered by the mask; this presents itself as a dark area that is visible in the reconstructed images in both the second and third experimental runs. This mask was chosen to ensure mask rigidity and structural integrity; however, Stephen Jesse has come up with several other mask designs that may be promising. At this point of the prototype, these different mask designs could all be easily tested as the masks can be printed off and switched with the masks currently inside of the ring gears. This would allow for an easy comparison and determination of the optimal mask design before final design completion.

Another improvement will come in the final design that was not present in this prototype: a motor encoder. The motor to be used in the final design has already been chosen and contains an encoder, which was not present in the cheaper motor used in the prototype design. An encoder would allow for a feedback loop to ensure exact positioning of the masks at each iteration. Overall, we successfully created an operational prototype that falls within the design constraints and allows for the implementation of compressive sensing techniques. The work presented here should allow for further testing to ensure successful compressive imaging using light followed by the creation of a similar device that will then be able to utilize these compressive sensing techniques to image material spectra using neutrons.

References

[1] B. S. Hudson, "Vibrational spectroscopy using inelastic neutron scattering: Overview and outlook," *Vibrational Spectroscopy,* vol. 42, no. 1, pp. 25-32, 2006/10/18/ 2006.
[2] A. Carden and M. D. Morris, "Application of vibrational spectroscopy to the study of mineralized tissues," *Journal of biomedical optics,* vol. 5, no. 3, pp. 259-269, 2000.
[3] D. L. Jeanmaire and R. P. Van Duyne, "Surface raman spectroelectrochemistry: Part I. Heterocyclic, aromatic, and aliphatic amines adsorbed on the anodized silver electrode," *Journal of Electroanalytical Chemistry and Interfacial Electrochemistry,* vol. 84, no. 1, pp. 1-20, 1977/11/10/ 1977.
[4] T. Vankeirsbilck *et al.*, "Applications of Raman spectroscopy in pharmaceutical analysis," *TrAC Trends in Analytical Chemistry,* vol. 21, no. 12, pp. 869-877, 2002/12/01/ 2002.
[5] S. Roy, J. R. Gord, and A. K. Patnaik, "Recent advances in coherent anti-Stokes Raman scattering spectroscopy: Fundamental developments and applications in reacting flows," *Progress in Energy and Combustion Science,* vol. 36, no. 2, pp. 280-306, 2010/04/01/ 2010.
[6] E. V. Efremov, F. Ariese, and C. Gooijer, "Achievements in resonance Raman spectroscopy: Review of a technique with a distinct analytical chemistry potential," *Analytica Chimica Acta,* vol. 606, no. 2, pp. 119-134, 2008/01/14/ 2008.
[7] R. S. Das and Y. K. Agrawal, "Raman spectroscopy: Recent advancements, techniques and applications," *Vibrational Spectroscopy,* vol. 57, no. 2, pp. 163-176, 2011/11/01/ 2011.
[8] S. Qaisar, R. M. Bilal, W. Iqbal, M. Naureen, and S. Lee, "Compressive sensing: From theory to applications, a survey," *Journal of Communications and networks,* vol. 15, no. 5, pp. 443-456, 2013.
[9] M. F. Duarte *et al.*, "Single-pixel imaging via compressive sampling," *IEEE signal processing magazine,* vol. 25, no. 2, pp. 83-91, 2008.
[10] J. van de Gronde and E. Vuçini, "Compressed sensing overview," ed, 2008.
[11] J. C. Schaake, R. C. Pooser, and S. Jesse, "Compressive Imaging with Stochastic Spatial Light Modulator," *arXiv preprint arXiv:1810.08694,* 2018.
[12] Pololu. (2018, 9 Oct.). *File downloads*. Available: https://www.pololu.com/product/3130/resources
[13] C. Li, W. Yin, and Y. Zhang. Available: https://www.caam.rice.edu/~optimization/L1/TVAL3/

Appendix

MATLAB: Sample Matrix Generation Code

```
%Daniel Garza
%UTK 2018
close all; clear all;

%sampling matrix file
file_name = 'Hypercool_Mask_25_bw-ConvertImage';

%name for output file
resultname = 'Hypercool_Sample_Matrix_2';

%creates directory for output if one does not exist
if ~exist('sample_matrices', 'dir');
    mkdir('sample_matrices');
end

plot_mask_configs_cond = 1; % plot mask configurations? 0 = no, 1 = yes,

%Reads in matrix file and creates logical
disk1 = imread([ file_name '.jpg'],'jpg');
disk1 = imbinarize(disk1);

%Rotates given file since starting position in experiment is 90 degrees
%different than file. Sets second disk to be the same as first disk
disk1 = imrotate(disk1,90,'crop');
disk2 = disk1;

%Individual mask rotations per step
dm1 = 12.5625;
dm2 = 12.9214;

count=0;
for cycle = 0:1:499

    %Rotates the disks at each iteration
    disk1rot = imrotate(disk1, cycle.*dm1,'crop');
    disk2rot = imrotate(disk2, cycle.*dm2,'crop');

    %Offsets the disks
    disk1pos = imtranslate(disk1rot,[0,-28]);
    disk2pos = imtranslate(disk2rot,[0,28]);

    %Puts the disks into the same matrix (image)
    double_disk = disk1pos.*disk2pos; %AP: elementwise (.*) matrix
      multiplication

        [ys,xs] = size(double_disk); %AP: number of rows and columns

        %Sets the aperture limits and crops away the matrix not within
            aperture
        %aperture limits were found via the relationship:
```

```
        %aperture length:mask diameter::aperture length(pixels):mask
            diameter(pixels)
        y_ap_max = round(ys/2)+353;
        y_ap_min = round(ys/2)-353;
        x_ap_max = round(xs/2)+212;
        x_ap_min = round(xs/2)-212;

        %For displaying aperture over disks
        figure(1)
        imshow(double_disk)
        hold on
        rectangle('Position',[x_ap_min y_ap_min (x_ap_max-x_ap_min)
            (y_ap_max-y_ap_min)],'EdgeColor', 'r','Linewidth',3)

        %The matrix visible in the aperture
        samp_mat = double_disk(y_ap_min:y_ap_max,x_ap_min:x_ap_max);

        %Displays and saves result
        disp(size(samp_mat))
        if(plot_mask_configs_cond)

             sample = count+1;
             imwrite(samp_mat,[resultname '_' num2str(sample) '.jpg' ]);

        end
        count=count+1;
end
```

Vita

Daniel Garza was raised in Maryville, TN, for the majority of his life, where he graduated from Maryville High School. After graduating in 2013, he attended the University of Tennessee and started a Bachelor of Science degree in Mechanical Engineering. During his senior year he began the 5-year master's program and took classes in both mechatronics and computational fluid dynamics. After graduating in the spring of 2017 with a minor in Materials Science and Engineering, he started work in Dr. Bill Hamel's robotics lab. During the first year of his graduate studies, he worked on a joint America Makes project proposed by Wolf Robotics. In this project the goal was to perform background research and evaluate the feasibility of performing additive manufacturing with multiple manipulators working together on a single part. Near the end of the summer of 2018, Daniel began work on the current project through Oak Ridge National Laboratory.